ADAPTIVE NEURAL NETWORK CONTROL FOR SMART MATERIALS ROBOTS USING SINGULAR PERTURBATION TECHNIQUE

S.S. Ge, T.H. Lee and Z.P. Wang

ABSTRACT

In this paper, an adaptive neural network controller is presented for smart materials robots using Singular Perturbation techniques by modeling the flexible modes and their derivatives as the fast variables and link variables as slow variables. The neural network (NN) controller is to control the slow dynamics in order to eliminate the need for the tedious dynamic modeling and the error prone process in obtaining the regressor matrix. In addition, inverse dynamic model evaluation is not required and the time-consuming training process is avoided except for initializing the NNs based on the approximate function values at the initial posture at time $t = 0$. The smart materials bonded along the links are used to active suppress the residue vibration. Simulation results have shown that the controller can control the system successfully and effectively.

KeyWords: Adaptive control, smart materials robots, neural networks, singular perturbation.

I. INTRODUCTION

For high speed positioning applications, light-weight manipulators are of considerable interest. With the promised advent of light-weight high strength composite materials, much attention has been given to modeling and control of flexible-link manipulators.

The control objective of a flexible robot system is often set as point-to-point position control or regulation, in which the main task is to suppress residue vibrations. Many approaches have been reported in the literature for such an objective, such as linear control [1], optimal control [2], sliding mode control [3], direct strain feedback control [4], and energy-based control [5]. Although the point-to-point position control is sufficient for certain applications, such as the automatic manufacturing assembly, it is more desirable to be able to drive the robot along a pre-defined trajectory.

The tracking control problem of flexible robots is often solved by converting the problem into two subproblems: (i) tracking of the joint motion (the dynamic behaviour of the system is of minimum phase, if the output is the joint angular position and the input is the torque at the joint), and (ii) suppression of the elastic vibrations of the flexible links. Such a consideration directly leads to a Singular Perturbation (SP) treatment [6]. The attractive feature of this strategy is that the slow control can be designed based on the well-established control schemes for rigid body manipulators, such as computed torque control [7], robust control [8] and adaptive control [9]. However, they rely on either the exact knowledge about the nonlinear functions, the knowledge of bounds of uncertainties, or the known nonlinear regression matrix of robots, which are not easy to obtain in practice. To remove these drawbacks, the approximation capabilities of neural networks have been utilized to approximate the nonlinear characteristics of the systems. The introduction of neural networks can remove the need for the tedious dynamic modeling and the error prone process in obtaining the regression matrix.

As there are an infinite number of degrees of freedom to be controlled, yet only a finite number of actuators are available for control action, there is a limit in further improving the control performance for conventional flexible link robots. The utilization of smart materials in control of flexible manipulators is receiving increased attention recently [10-12].

In this paper, we shall investigate the problem of adaptive neural network control for a smart materials flexible robot where a finite number of segmented piezoelectric patches are bonded along links. Singular perturbed model of the system is derived which allow the controller design be split into two separate controller designs for the two reduced-order subsystems. The adap-

Manuscript received September 13, 2000; revised February 7, 2001; accepted March 29, 2001.

The authors are with Department of Electrical and Computer Engineering, National University of Singapore, Singapore 117576.

tive neural network controller for slow dynamics eliminates the need for the tedious dynamic modeling and the error prone process in obtaining the regressor matrix. For the stabilization of the fast subsystem, active vibration control using smart materials voltage is considered, which turns out to be independent of the unknown dynamics of the system. Since the design of joint torque control for the fast subsystem depends on the unknown dynamics of the system, it is dropped in the stabilization of the fast system.

The paper is organized as follows. In Section 2, the problems of NN approximation is briefly introduced. The singular perturbed model of smart materials robots is presented in Section 3. In Section 4, adaptive NN composite controller design is presented for the smart materials robotic system. Numerical simulations are given in Section 5 to show the effectiveness of the proposed controller.

II. NEURAL NETWORK STRUCTURE

Neural networks have been widely used in modeling and control of nonlinear systems because of their good capabilities of nonlinear function approximation, learning and fault tolerance. The feasibility of applying NNs to dynamic system control has been demonstrated in many studies [13-16]. In control engineering, an NN is usually used to generate input/output maps using the property that a multi-layer neural network can approximate any function, under mild assumptions, with any desired accuracy. There are two distinct problems in function approximation, namely, the *representation problem* of choosing the best approximating function $\hat{f}(\psi, x)$ for a given function $f(x)$, and the *learning problem* of finding the training method to obtain the optimal parameters ψ^*.

The adaptive NN portion of the proposed controller utilizes controller parameterization techniques coupled with methods of direct adaptive control. Thus, the architecture of the NNs has to be chosen such that it can be linearly parameterized (*representation problem*) and direct adaptive laws can be used to update the parameters of the networks on-line (*learning problem*) [15]. The RBF network is most suitable for this application.

It has been demonstrated in [17] that a linear superposition of Gaussian RBFs results in an optimal mean square approximation to an unknown function which is infinitely differentiable and whose values are specified at a finite set of points in $\mathcal{R}^n$. Further, it has been proven in [18] that any continuous function, not necessarily infinitely smooth, can be uniformly approximated by a linear combination of Gaussian RBFs.

The Gaussian RBF neural network is a particular network architecture [18] utilizing k numbers of Gaussian radial basis functions (activation functions), $a_i(q)$, with input variables $q \in R^n$, variance $\sigma^2 \in R$ and the center vector $c = (c_1, \ldots, c_n)^T \in R^n$. Gaussian radial functions are particularly attractive: they are bounded, strictly positive and absolutely integrable on R^n, and further, they are their own Fourier transforms. Hence, for any given function, $y = f(q)$, it can be approximated by a Gaussian RBF neural network expressed as

$$y = W^T a(q) + \epsilon \quad (1)$$

$$a_i(q) = \exp\left(-\frac{\|q-c\|^2}{\sigma^2}\right) = \exp\left(-\frac{(q-c)^T(q-c)}{\sigma^2}\right) \quad (2)$$

where $W^T = [w_{ij}]$, $a = [a_1\ a_2\ \ldots\ a_k]^T$, $y \in R_n$ and ϵ is the NN reconstruction error.

III. SINGULAR PERTURBED SMART MATERIALS ROBOTS

Smart materials robots retain the benefit of the flexible link robots and at the same time have additional sensoring and control abilities via the piezoelectric materials bonded/embedded along the links. Different approaches such as Assumed Modes Method (AMM) [19] and Finite Element Method (FEM) [19] can be utilized to model smart materials robots.

For those robots that are either operated in the horizontal plane or deployed in space, the effect of gravity is ignored. Using AMM, we can obtain the dynamics of smart materials robots as follows

$$M(q)\ddot{q} + C(q,\dot{q})\dot{q} + Kq = Fu \quad (3)$$

where

1. $q = [q_r^T\ q_f^T]^T \in \mathcal{R}^n$, $n = n_f + n_r$, with $q_r \in \mathcal{R}^{n_r}$ the vector of the rigid variables and $q_f \in \mathcal{R}^{n_f}$ the vector of the flexible variables;
2. $M(q) \in \mathcal{R}^{n \times n}$ is the symmetric positive definite inertia matrix;
3. $C(q, \dot{q})\dot{q} \in \mathcal{R}^n$ represents the Coriolis and Centrifugal forces;
4. $K \in \mathcal{R}^{n \times n}$ is the stiffness matrix of the smart materials robot;
5. $u = [\tau\ w]^T$ is the vector of generalized torque with $\tau \in \mathcal{R}^{n_r}$ the vector of joint control torques, $w \in \mathcal{R}^m$ the vector of the control voltages to the piezoelectric materials where m is the number of the piezoelectric materials actuators, and $F = diag[I,\ F_f]$ with $I \in \mathcal{R}^{n_r \times n_r}$ is an identity matrix and $F_f \in \mathcal{R}^{n_f \times m}$ is of full row rank.

Note that the model obtained using AMM can guarantee that F_f is of full row rank. On the other hand, it is not necessarily true when FEM is used in dynamic modeling.

Exploiting the natural time-scale separation between the faster flexible mode dynamics and the slower desired rigid mode dynamics, we use singular perturbation theory to formulate a boundary layer correction that stabilizes non-minimum phase internal dynamics. Dynamic equation (3) can be partitioned as

$$\begin{bmatrix} M_{rr} & M_{rf} \\ M_{fr} & M_{ff} \end{bmatrix}\begin{bmatrix} \ddot{q}_r \\ \ddot{q}_f \end{bmatrix}+\begin{bmatrix} H_r \\ H_f \end{bmatrix}+\begin{bmatrix} 0 \\ K_{ff}q_f \end{bmatrix}=\begin{bmatrix} \tau \\ F_f w \end{bmatrix} \quad (4)$$

where

$$H_r=C_{rr}\dot{q}_r+C_{rf}\dot{q}_f$$

$$H_f=C_{fr}\dot{q}_r+C_{ff}\dot{q}_f$$

It should be noted that $\dot{M}-2C$ is skew-symmetric as in the rigid robot case. Correspondingly, $\dot{M}_{rr}-2C_{rr}$ is also skew-symmetric. Since inertia matrix M is positive definite, its inverse exists and is denoted by D as

$$M^{-1}=D=\begin{bmatrix} D_{rr} & D_{rf} \\ D_{fr} & D_{ff} \end{bmatrix} \quad (5)$$

where

$$D_{rr}=(M_{rr}-M_{rf}M_{ff}^{-1}M_{fr})^{-1} \quad (6)$$

$$D_{rf}=-M_{rr}^{-1}M_{rf}(M_{ff}-M_{fr}M_{rr}^{-1}M_{rf})^{-1} \quad (7)$$

$$D_{fr}=-M_{ff}^{-1}M_{fr}(M_{rr}-M_{rf}M_{ff}^{-1}M_{fr})^{-1} \quad (8)$$

$$D_{ff}=(M_{ff}-M_{fr}M_{rr}^{-1}M_{rf})^{-1} \quad (9)$$

Solving Equation (4) for $\ddot{q}_r$ and $\ddot{q}_f$ yields

$$\ddot{q}_r=-D_{rr}H_r-D_{rf}H_f-D_{rf}K_{ff}q_f+D_{rr}\tau+D_{rf}F_f w \quad (10)$$

$$\ddot{q}_f=-D_{fr}H_r-D_{ff}H_f-D_{ff}K_{ff}q_f+D_{fr}\tau+D_{ff}F_f w \quad (11)$$

Introducing an appropriate scale factor k such that

$$K_{ff}=k\tilde{K} \quad (12)$$

The following new variables can be defined as $\xi := k\tilde{K}q_f$. Now define $\epsilon^2 := 1/\text{k}$, equations (10) and (11) become

$$\begin{aligned}\ddot{q}_r=&-D_{rr}(q_r,\epsilon^2\xi)H_r(q_r,\dot{q}_r,\epsilon^2\xi,\epsilon^2\dot{\xi})\\&-D_{rf}(q_r,\epsilon^2,\xi)H_f(q_r,\dot{q}_r,\epsilon^2\xi,\epsilon^2\dot{\xi})\\&-D_{rf}(q_r,\epsilon^2\xi)\xi+D_{rr}(q_r,\epsilon^2\xi)\tau+D_{rf}(q_r,\epsilon^2\xi)F_f w\end{aligned} \quad (13)$$

$$\begin{aligned}\epsilon^2\ddot{\xi}=&-D_{fr}(q_r,\epsilon^2\xi)H_r(q_r,\dot{q}_r,\epsilon^2\xi,\epsilon^2\dot{\xi})\\&-D_{ff}(q_r,\epsilon^2,\xi)H_f(q_r,\dot{q}_r,\epsilon^2\xi,\epsilon^2\dot{\xi})\\&-D_{ff}(q_r,\epsilon^2\xi)\xi+D_{fr}(q_r,\epsilon^2\xi)\tau+D_{ff}(q_r,\epsilon^2\xi)F_f w\end{aligned} \quad (14)$$

which is a singular perturbed model of the smart materials robot arm. Notice that all variables on the right hand sides of (13) and (14) have been scaled by $\tilde{K}$. Formally, setting $\epsilon=0$ and solving for ξ in (14), we obtain

$$\begin{aligned}\bar{\xi}=&D_{ff}^{-1}(\bar{q}_r,0)[-D_{fr}(\bar{q}_r,0)H_r(\bar{q}_r,\dot{\bar{q}}_r,0,0)+D_{fr}(\bar{q}_r,0)\bar{\tau}]\\&-H_f(\bar{q}_f,0)+F_f\bar{w}\end{aligned} \quad (15)$$

where the overbars are used to indicate that the system is considered with $\epsilon=0$. Substitute (15) into (13) with $\epsilon=0$ yields

$$\begin{aligned}\ddot{\bar{q}}_r=&[D_{rr}(\bar{q}_r,0)-D_{rf}(\bar{q}_r,0)D_{ff}^{-1}(\bar{q}_r,0)D_{fr}(\bar{q}_r,0)]\\&[-H_r(\bar{q}_r,\dot{\bar{q}}_r,0,0)+\bar{\tau}]\end{aligned} \quad (16)$$

Utilizing the expressions (6)-(9) yields

$$D_{rr}(\bar{q}_r,0)-D_{rf}(\bar{q}_r,0)D_{ff}^{-1}(\bar{q}_r,0)D_{fr}(\bar{q}_r,0)=M_{rr}^{-1}(\bar{q}_r) \quad (17)$$

Thus, equation (16) becomes

$$M_{rr}(\bar{q}_r)\ddot{\bar{q}}_r+C_{rr}(\bar{q}_r,\dot{\bar{q}}_r)\dot{\bar{q}}_r=\bar{\tau} \quad (18)$$

which corresponds to the rigid body robot dynamic model.

Remark 3.1 It can be seen that $\bar{w}$ does not appear in equation (16), it means that the voltage control w has no influence on the slow subsystem, thus, $\bar{w}=0$. It coincides with the physical function of the voltage control of the smart materials robots.

To identify the fast subsystem, define a fast time scale $\tau_t=t/\epsilon$ and boundary layer correction variables $z_1=\xi-\bar{\xi}$ and $z_2=\epsilon\dot{\xi}$. From (14) and the fact that $d\bar{\xi}/d\tau_t=\epsilon\dot{\bar{\xi}}=0$, we have

$$\frac{dz_1}{d\tau_t}=z_2 \quad (19)$$

$$\begin{aligned}\frac{dz_2}{d\tau_t}=&-D_{fr}(q_r,\epsilon^2(z_1+\bar{\xi}))H_r(q_r,\dot{q}_r,\epsilon^2(z_1+\bar{\xi}),\epsilon z_2)\\&-D_{ff}(q_r,\epsilon^2(z_1+\bar{\xi}))H_f(q_r,\dot{q}_r,\epsilon^2(z_1+\bar{\xi}),\epsilon z_2)\\&-D_{ff}(q_r,\epsilon^2(z_1+\bar{\xi}))(z_1+\bar{\xi})+D_{fr}(q_r,\epsilon^2(z_1+\bar{\xi}))\tau\\&+D_{ff}(q_r,\epsilon^2(z_1+\bar{\xi}))F_f w\end{aligned} \quad (20)$$

Setting $\epsilon = 0$, and substituting for $\bar{\xi}$ from (15) results in

$$\frac{dz_1}{d\tau_t} = z_2 \quad (21)$$

$$\frac{dz_2}{d\tau_t} = -D_{ff}(\bar{q}_r, 0)z_1 + D_{fr}(\bar{q}_r + 0)\tau_f + D_{ff}(\bar{q}_r, 0)F_f w \quad (22)$$

which is a linear system parameterized in the slow variable $\bar{q}_r$ and $\tau_f = \tau - \bar{\tau}$.

IV. COMPOSITE CONTROL OF SMART MATERIALS ROBOTS

As shown in the previous section, using the singular perturbation theory, the full system can be modeled as two subsystems: linear fast dynamics (21)-(22) and nonlinear slow dynamics (18). Therefore, a composite control strategy can be pursued. The main control objective is to let the rigid motion $q_r(t)$ track a desired trajectory $q_d(t)$ and at the same time provide active damping to the flexible motion of the flexible links.

4.1 Adaptive NN control for slow subsystem

Given a desired trajectory $q_d(t) \in \mathcal{R}^{n_r}$ which is twice differentiable for the slow part of the flexible link dynamics, the tracking error is

$$e = q_d - \bar{q}_r \quad (23)$$

$$\dot{q}_v = \dot{q}_d + \Lambda e \quad (24)$$

$$r = \dot{q}_v - \dot{\bar{q}}_r = \dot{e} + \lambda e \quad (25)$$

where Λ is a symmetric positive definite matrix.

Differentiating $r(t)$ and using (18), the dynamic equation can be written in term of the new tracking measure r as

$$M_{rr}(\bar{q}_r)\dot{r} = -C_{rr}(\bar{q}_r, \dot{\bar{q}}_r)r - \bar{\tau} + M_{rr}(\bar{q}_r)\ddot{q}_v + C_{rr}(\bar{q}_r, \dot{\bar{q}}_r)\dot{q}_v \quad (26)$$

Now, consider the general controller of the form

$$\bar{\tau} = \hat{M}_{rr}\ddot{q}_v + \hat{C}_{rr}\dot{q}_v + K_p r + K_s sgn(r) \quad (27)$$

where $(\hat{*})$ be the estimate of $(*)$ and the estimation error given as $(\tilde{*}) = (*) - (\hat{*})$, $K_p > 0$, K_s will be designed later.

Using NN, $m_{ij}(\bar{q}_r)$ and $c_{ij}(\bar{q}_r, \dot{\bar{q}}_r)$ can be approximated as

$$m_{ij}(\bar{q}_r) = \psi_{ij}^T \delta_{ij}(\bar{q}_r) + \epsilon_{M_{ij}} \quad (28)$$

$$c_{ij}(\bar{q}_r, \dot{\bar{q}}_r) = \alpha_{ij}^T \zeta_{ij}(\bar{q}_r, \dot{\bar{q}}_r) + \epsilon_{C_{ij}} \quad (29)$$

where ψ_{ij}, α_{ij} are the weight vectors; $\delta_{ij}(\bar{q}_r)$, $\zeta_{ij}(\bar{q}_r, \dot{\bar{q}}_r)$ are Gaussian RBFs; and $\epsilon_{M_{ij}}$, $\epsilon_{C_{ij}}$ are the NN reconstruction errors respectively.

Using the notation for "GL" matrix and operator [15], the function emulators (28)-(29) can be collectively expressed as

$$M_{rr}(\bar{q}_r) = [\{\Psi\}^T \bullet \{\Delta\}] + E_M \quad (30)$$

$$C_{rr}(\bar{q}_r, \dot{\bar{q}}_r) = [\{A\}^T \bullet \{Z\}] + E_C \quad (31)$$

where $[\{\Psi\}, \{\Delta\}]$ and $[\{A\}, \{Z\}]$ are the desired parameter and basis function pairs of the NN emulation of $M_{rr}(\bar{q}_r)$, $C_{rr}(\bar{q}_r, \dot{\bar{q}}_r)$ respectively; and E_M, E_C are the collective NN reconstruction errors respectively.

Now, the estimates $(\hat{*})$ required in (27) be provided by NN so that

$$\hat{M}_{rr}(\bar{q}_r) = [\{\hat{\Psi}\}^T \bullet \{\Delta\}] \quad (32)$$

$$\hat{C}_{rr}(\bar{q}_r, \dot{\bar{q}}_r) = [\{\hat{A}\}^T \bullet \{Z\}] \quad (33)$$

Substituting (27) and (32)-(33) into (26) yields the closed-loop system error equation

$$M_{rr}\dot{r} + C_{rr}r + K_p r + K_s sgn(r)$$
$$= [\{\tilde{\Psi}\}^T \bullet \{\Delta\}]\ddot{q}_v + [\{\tilde{A}\}^T \bullet \{Z\}]\dot{q}_v + E \quad (34)$$

where $E = E_M\ddot{q}_v + E_C\dot{q}_v$.

The stability of the closed-loop system (34) are given by the following theorem.

Theorem 4.1 For a closed-loop system given in (34), asymptotic stability, i.e., $r \to 0$ as $t \to \infty$, is achieved if $K_p > 0$, $K_s \geq \| E \|$ and the parameter adaptation laws are given by

$$\dot{\hat{\psi}}_i = \Gamma_i \bullet \{\delta_i\}\ddot{q}_v r_i \quad (35)$$

$$\dot{\hat{\alpha}}_i = W_i \bullet \{\zeta_i\}\dot{q}_v r_i \quad (36)$$

where Γ_i and W_i are dimensional compatible symmetric positive definite matrices, then $\hat{\psi}_i$, $\hat{\alpha}_i \in L^\infty$; and $e \in L_n^2 \cap L_n^\infty$; $\dot{e} \in L_n^2$, e is continuous and e, $\dot{e} \to 0$ as $t \to \infty$.

Proof. See [14].

4.2 Active stabilization of fast subsystem

Though flexible manipulators have advantages in terms of speed, mobility and reduced energy consumption, their vibrational characteristics make control more difficult. Passive damping of flexible robot arm is not adequate due to its additional mass and its inability to adjust to changing flexibility effects. Hence, some kind of active damping is desired to control the vibrations.

Examining the fast subsystem (21) and (22), it can be seen that there are two kinds of control inputs τ_f and w to stabilize the fast variables, z. However, the design of τ_f is difficult because (i) the dynamics of the system are assumed to be unknown, and (ii) there is no nice property about $D_{fr}(\bar{q}_r, 0)$ can be used. Fortunately, for the design of voltage control w, we can fully utilize the positivity of $D_{ff}(\bar{q}_r, 0)$ to design a controller which is independent of the unknown dynamics yet stabilizes the fast subsystem. Thus, we shall investigate the scheme where the slow subsystem is controlled by $\bar{\tau}$, and the fast subsystem is controller by w only by choosing $\tau_f = 0$ in this paper.

By letting $\tau_f = 0$, the fast subsystem reduces to

$$\frac{d^2 z_1}{d\tau_t^2} + D_{ff}(\bar{q}_r, 0) z_1 = D_{ff}(\bar{q}_r, 0) F_f w \tag{37}$$

where $D_{ff}(\bar{q}_r, 0)$ is positive definite and F_f is an known full row rank matrix.

Theorem 4.2 For the fast subsystem (37), if F_f is a full row rank matrix and known, then system (37) is uniform exponential stable if the control is chosen as

$$w = -\epsilon k U F_f^+ \dot{\xi}, \quad k > 0 \tag{38}$$

where U is the permutation matrix such that $F_f U = [F_{f1} \; F_{f2}]$ with $F_{f1} \in R^{n_f \times n_f}$ is non-singular, and the right inverse F_f^+ is, for any dimensionally compatible matrix F_{f3}, given by [20]

$$F_f^+ = \begin{bmatrix} F_{f1}^{-1} - F_{f1}^{-1} F_{f2} F_{f3} \\ F_{f3} \end{bmatrix} \tag{39}$$

Proof. Consider the Lyapunov function candidate

$$V = \frac{1}{2} z_1'^T z_1' + \frac{1}{2} z_1^T D_{ff}(\bar{q}_r, 0) z_1 \tag{40}$$

where z_1' denotes $dz_1/d\tau_t$.

Since $\bar{\xi}$ is considered constant in the boundary layer, control law (38) can be rewritten in the fast time scale as

$$w = -\epsilon k U F_f^+ \dot{z}_1 = -k U F_f^+ z_1' \tag{41}$$

Substituting (41) into the fast subsystem, we have

$$\frac{d^2 z_1}{d\tau_t^2} + k D_{ff}(\bar{q}_r, 0) F_f U F_f^+ \frac{dz_1}{d\tau_t} + D_{ff}(\bar{q}_r, 0) z_1 = 0 \tag{42}$$

By noting $F_f U = [F_{f1} \; F_{f2}]$ where $F_{f1} \in R^{n_f \times n_f}$ is non-singular, and its right inverse F_f^+ is given by (39), we know that $F_f U F_f^+ = I$. Thus, equation (42) becomes

$$\frac{d^2 z_1}{d\tau_t^2} + k D_{ff}(\bar{q}_r, 0) \frac{dz_1}{d\tau_t} + D_{ff}(\bar{q}_r, 0) z_1 = 0 \tag{43}$$

Accordingly, along trajectory (43), we have

$$\frac{dV}{d\tau_t} = -k z_1'^T D_{ff}(\bar{q}_r, 0) z_1' \le 0 \tag{44}$$

Global asymptotic stability of the boundary layer system (42) then follows from LaSalles's Theorem. Since the system is linear and it is uniform in $\bar{q}_r$, the fast subsystem is exponentially uniformly stable for fixed $\bar{q}_r$. ■

Under these conditions, the following statements can be made based on Tikhonov's theorem.

If the slow subsystem (18) has a unique solution defined on an interval $t \in [0, t_1]$ and if the fast subsystem (37) is exponentially uniformly stable in $(t, \bar{q}_r)$, there exists ϵ^* such that for all $\epsilon < \epsilon^*$

$$\xi(t) = \bar{\xi}(t) + z_1(\tau_t) + O(\epsilon) \tag{45}$$

$$q_r(t) = \bar{q}_r(t) + O(\epsilon) \tag{46}$$

hold uniformly for $t \in [0, t_1]$.

Remark 4.1 When the system model is known, then both τ_f and w can be used to control the fast subsystem. In this case, the fast subsystem can be written as

$$\frac{dz}{d\tau_t} = Az + B_1 u_f \tag{47}$$

where $z = [z_1^T \; z_2^T]^T$ and

$$A = \begin{bmatrix} 0 & I \\ -D_{ff}(\bar{q}_r, 0) & 0 \end{bmatrix}, \; B_1 = \begin{bmatrix} 0 & 0 \\ D_{fr}(\bar{q}_r, 0) & D_{ff}(\bar{q}_r, 0) F_f \end{bmatrix},$$

$$u_f = \begin{bmatrix} \tau_f \\ w \end{bmatrix} \tag{48}$$

By examining the equation (47), we can find that there are two kinds of control inputs τ_f and w can be used to suppress the vibrations, z.

If w is unavailable or not activated, the fast subsystem becomes

$$\frac{dz}{d\tau_t} = Az + B_2 \tau_f \tag{49}$$

Table 1. System parameters.

names	symbols (unit)	values
pure beam thickness	$a(m)$	0.008
piezoelectric actuator thickness	$c_1(m)$	0.0008
piezoelectric sensor thickness	$c_2(m)$	0.0004
width of the beam	$b(m)$	0.01
length of the piezoelectric material	$l(m)$	0.01
length of the beam	$L(m)$	1
density of the pure beam	$\rho_1(kg/m)$	0.1
density of the piezoelectric material	$\rho_2(kg/m^3)$	1800
moment inertia of the hub	$I_h(kgm^2)$	3.0
tip payload	$m_3(kg)$	0.001
stiffness of the beam	$c_{11}^m(N/m^2)$	6×10^8
stiffness of the piezoelectric material	$c_{11}^s(N/m^2)$	8×10^6
permeability of the piezoelectric material	$\mu^{33}(H/m)$	1.2×10^{-6}
coupling parameter	$h_{12}(V/m)$	5×10^{11}
impermittivity	$\beta_{22}(m/F)$	4×10^{14}

where

$$A=\begin{bmatrix}0 & I\\ -D_{ff}(\bar{q}_r,0) & 0\end{bmatrix},\ B_2=\begin{bmatrix}0\\ D_{f_r}(\bar{q}_r,0)\end{bmatrix} \tag{50}$$

If τ_f is not used, the fast subsystem becomes

$$\frac{dz}{d\tau_t}=Az+B_3w \tag{51}$$

where

$$A=\begin{bmatrix}0 & I\\ -D_{ff}(\bar{q}_r,0) & 0\end{bmatrix},\ B_3=\begin{bmatrix}0\\ D_{ff}(\bar{q}_r,0)F_f\end{bmatrix} \tag{52}$$

Under the assumptions that pairs (A, B_2), (A, B_3) and hence (A, B_1) are uniformly stabilizable for any slow trajectory $\bar{q}_r(t)$, different linear control strategies such as LQR and pole placement methods can be used to design the fast feedback control law $u_f = Kz$ to make the fast subsystem uniform exponential stable.

V. SIMULATION TESTS

To verify its effectiveness, numerical simulations are carried out for a single-link smart materials robot operating in the horizontal plane. The smart materials robot is simulated using a 4 modes dynamic model (See Appendix A for detailed derivation). A fourth-order Runge-Kutta program with adaptive-step-size is used to numerically solve the ODEs [15]. The sampling interval is set to be 0.005s.

5.1 Trajectory planning

The desired trajectory for rigid joint angle is expressed as a Hermite polynomial of the fifth degree in t with continuous bounded position, velocity and bounded acceleration. The general expression for the desired position trajectory is:

$$q_d(t,t_d)=q_0+\left(6.0\frac{t^5}{t_d^5}-15\frac{t^4}{t_d^4}+10.0\frac{t^3}{t_d^3}\right)(q_f-q_0) \tag{53}$$

t_d represents the time that the desired arm trajectory reaches the desired final position q_f starting from the desired initial position q_0. In this paper, $q_0 = 0.0$, $q_f = 1.0$ and $t_d = 2.0$ seconds.

It has been shown that the simple joint PD control can stabilize the flexible robots [21], therefore, we will show the performance of PD controller first. When the weight adaptations (35)-(36) of the neural network controller were not activated, i.e., $\Gamma_i = 0$ and $W_i = 0$, the controller (27) becomes the traditional PD controller, it is given by PD:

$$\bar{\tau}=K_pr=K_p\dot{e}+K_ee \tag{54}$$

The adaptive NN composite controller for simulation is given by ANNC:

$$u=\begin{bmatrix}\tau\\ w\end{bmatrix}=\begin{bmatrix}\bar{\tau}\\ w\end{bmatrix}=\begin{bmatrix}\hat{M}_{rr}\ddot{q}_v+\hat{C}_{rr}\dot{q}_v+K_p r+K_s\mathrm{sgn}(r)\\ -\epsilon k K_w\dot{\xi}\end{bmatrix} \tag{55}$$

where

$$\begin{bmatrix}\hat{M}_{rr}(\bar{q}_r)\\ \hat{C}_{rr}(\bar{q}_r,\dot{\bar{q}}_r)\end{bmatrix}=\begin{bmatrix}[\{\hat{\Psi}\}^T\bullet\{\Delta\}]\\ [\{\hat{A}\}^T\bullet\{Z\}]\end{bmatrix}\quad\begin{bmatrix}\dot{\hat{\psi}}_i\\ \dot{\hat{\alpha}}_i\end{bmatrix}=\begin{bmatrix}\Gamma_i\bullet\{\delta_i\}\ddot{q}_v r_i\\ W_i\bullet\{\zeta_i\}\dot{q}_v r_i\end{bmatrix} \tag{56}$$

For both controllers, the following parameters were chosen as $K_p = 10$, $\lambda = 5$, while K_s was set to zero in order to test the robustness of the proposed controller. For the element of $\hat{M}$, 50 nodes static networks were chosen, while 200 nodes dynamic networks were chosen for the elements of $\hat{C}$, and $\mu = 0$, $\sigma^2 = 10$. The weight adaptations (35)-(36) of the neural network controller were activated by $\Gamma_i = 0.5$ and $W_i = 0.1$. To test the effectiveness of the proposed controller, only one pair of piezoelectric actuator and sensor is used in the simulation. The pair of piezoelectric patches are located at $x = 0.1$L of the beam. Hence, only the first mode's shape function was used in the controller design, and $kK_w = -500$ to make $kD_{ff}(\bar{q}_r, 0)\, F_f K_w$ positive definite.

Figure 1 shows the joint angle trajectory under PD and ANNC control. It can be seen that PD control gives worse performance whereas ANNC can make the joint angle track the desired trajectory quickly and smoothly. Fig. 2 shows the tip deflections of the smart materials robot by using PD and ANNC controllers. It can be seen that the tip deflections under ANNC converge faster than that under PD control. ANNC can suppress the vibration effectively, there is no residue vibration at steady state for ANNC. By utilizing the smart materials, active vibration damping are applied to the system and better control performances can be obtained.

What we care about most is the trajectory of the tip. The tip is required to track the desired trajectory fast with as small residual vibration/overshoot as possible to improve positioning accuracy. Under the assumption of small deflection, the tip position of the robot can be approximated by

$$pt = L\theta(t) + w(L, t) \tag{57}$$

where p_t is the tip position, $w(L, t)$ is the tip deflection of the smart materials robot and the angular position should be represented in radians instead of degrees. The tip positions under different controllers are depicted in Fig. 3. It can be seen that the tip position of the ANNC can converge faster than that of the PD and there is no residue vibration at steady state for ANNC.

For completeness and clarity in presentation, other signals in the closed-loop are included. Figure 4 shows the bounded joint control torque signals under both controllers, while Fig. 5 shows the control voltages in ANNC.

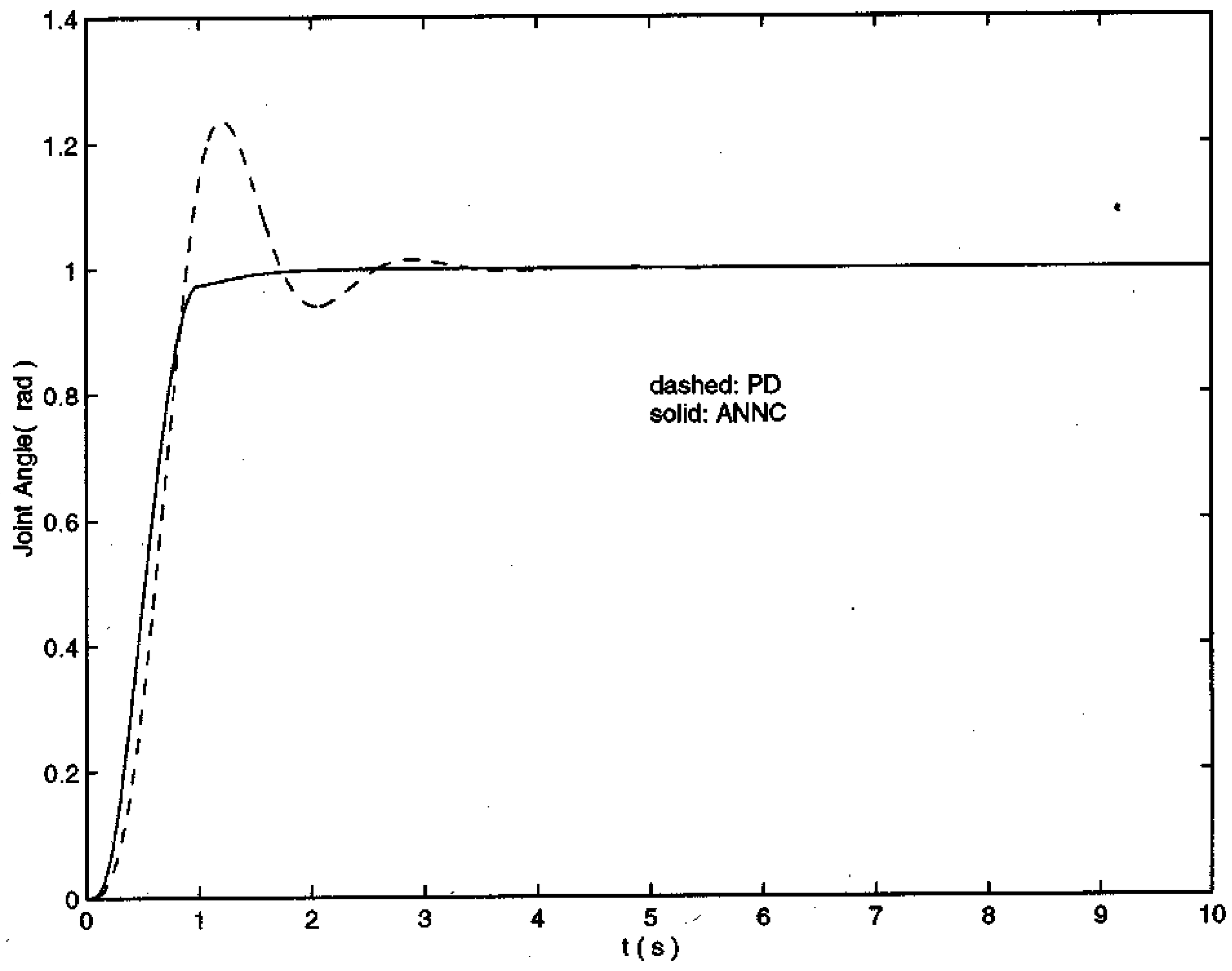

Fig. 1. Joint angle trajectory of PD and ANNC.

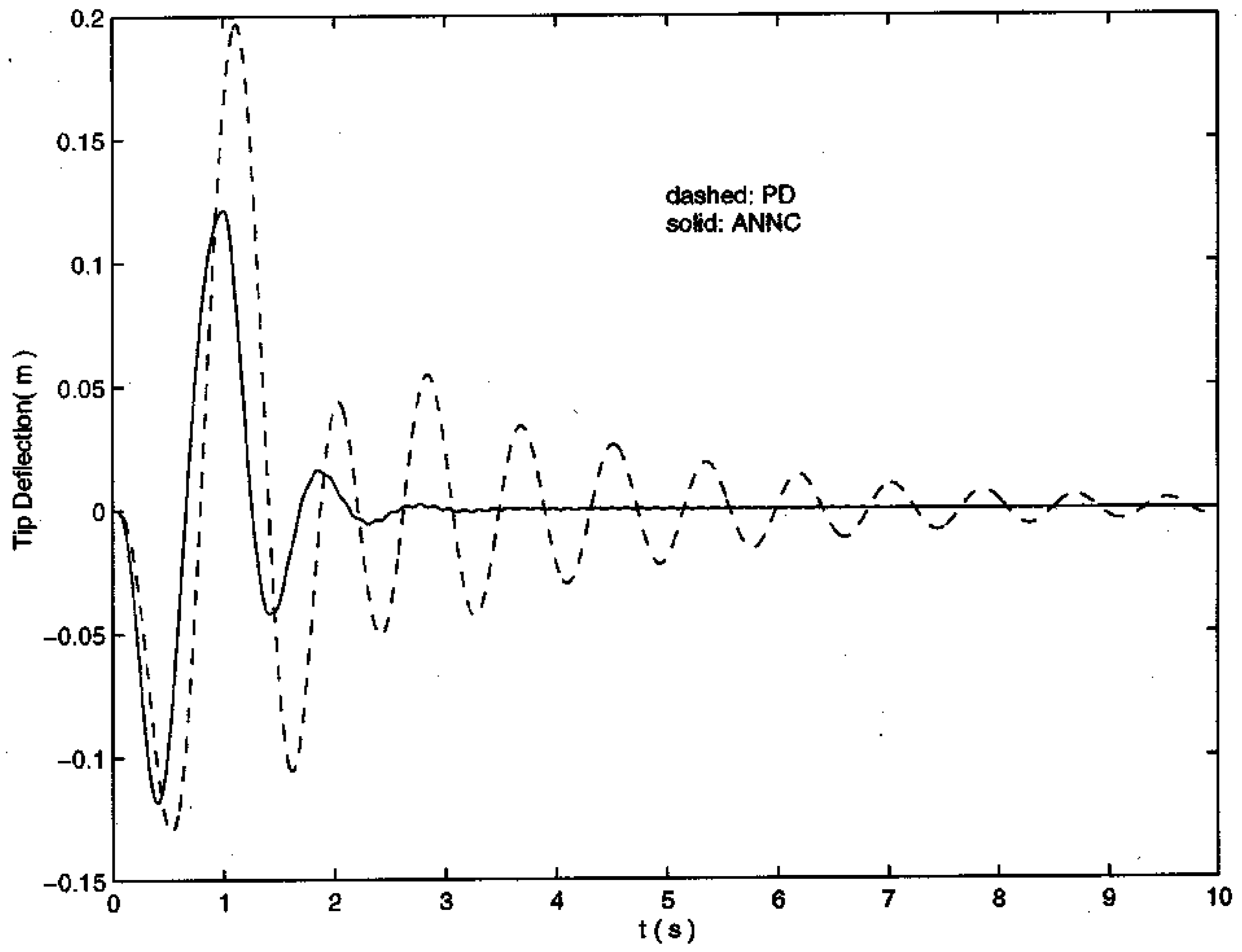

Fig. 2. Tip deflections of PD and ANNC.

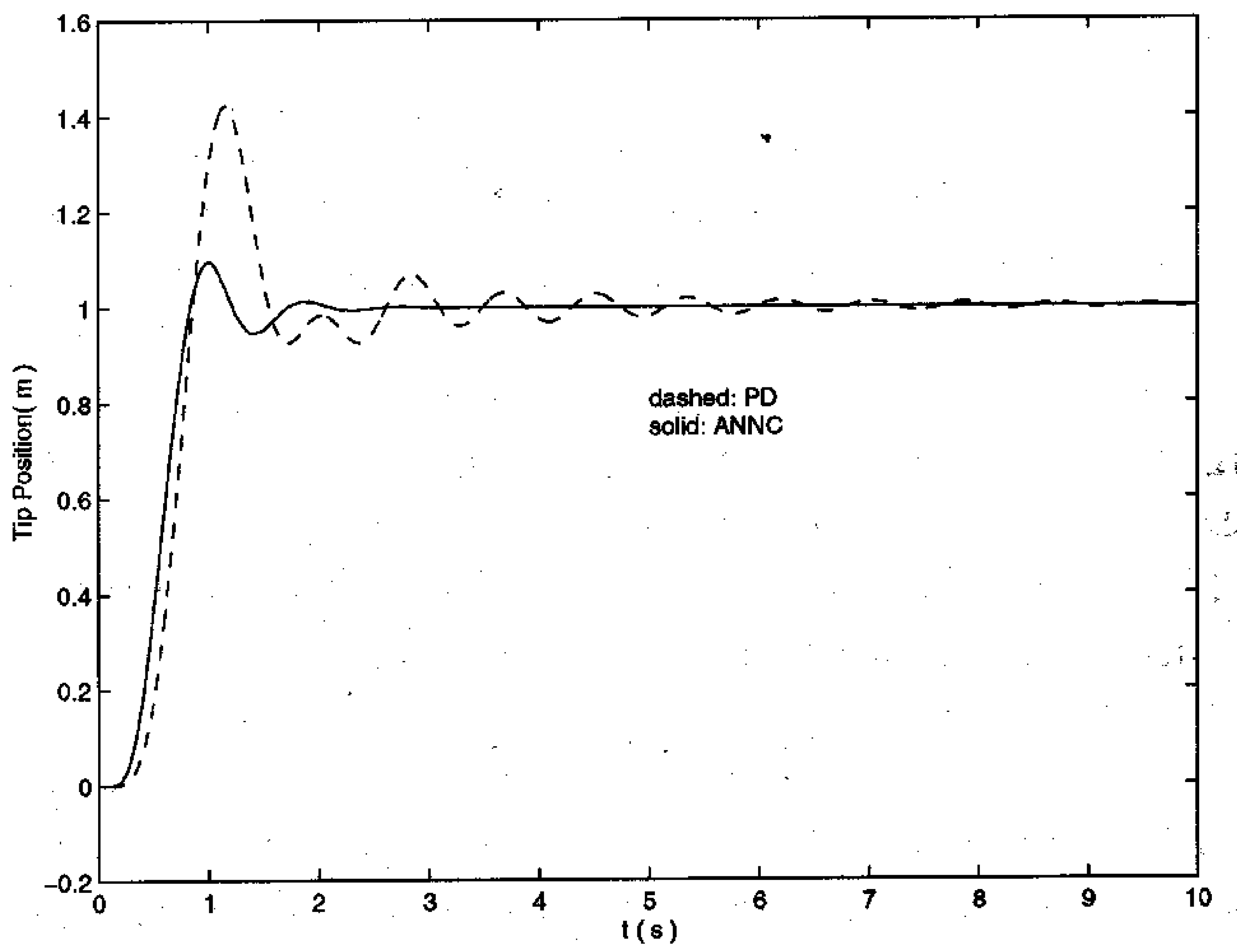

Fig. 3. Tip position trajectory of PD and ANNC.

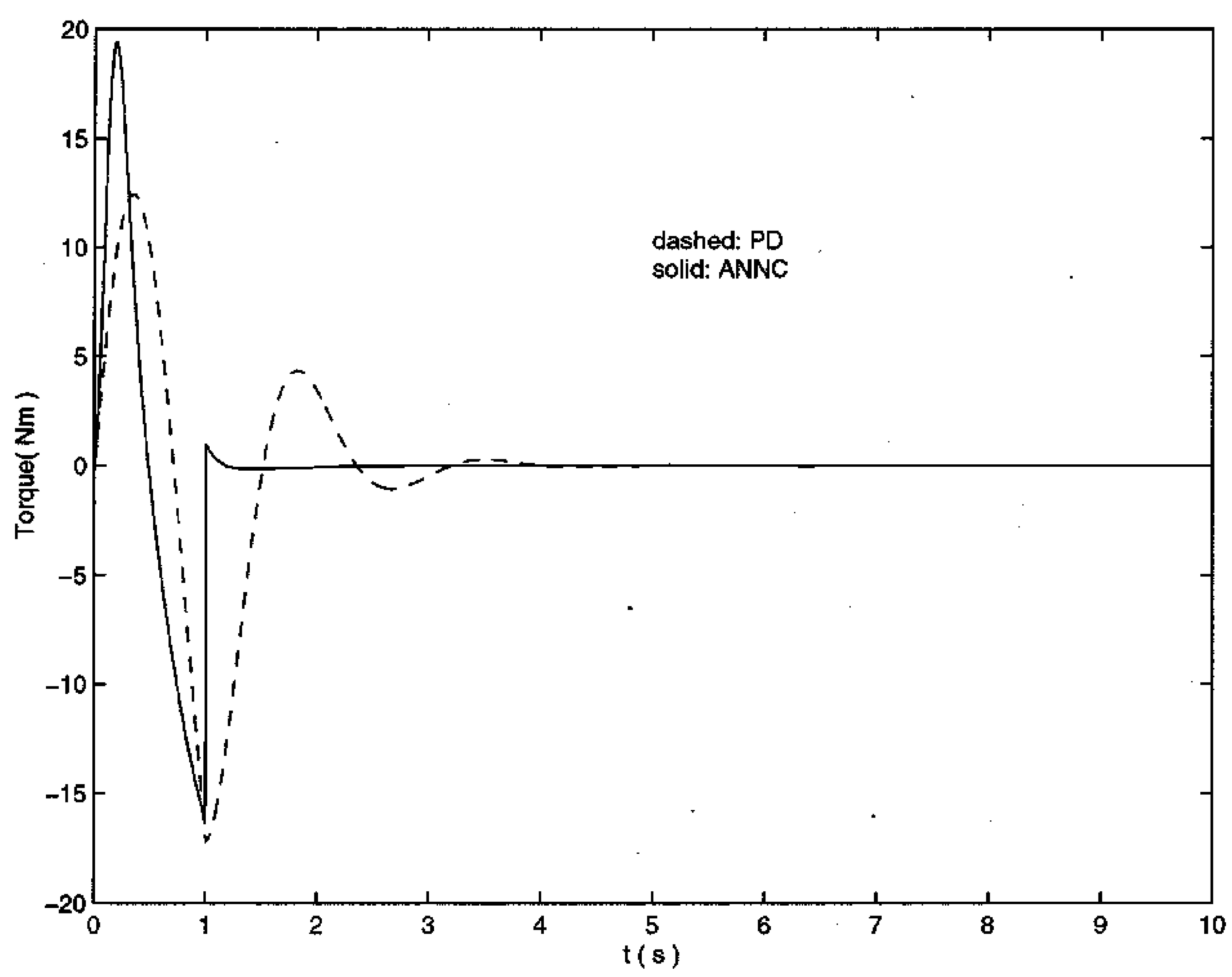

Fig. 4. Torque control of PD and ANNC.

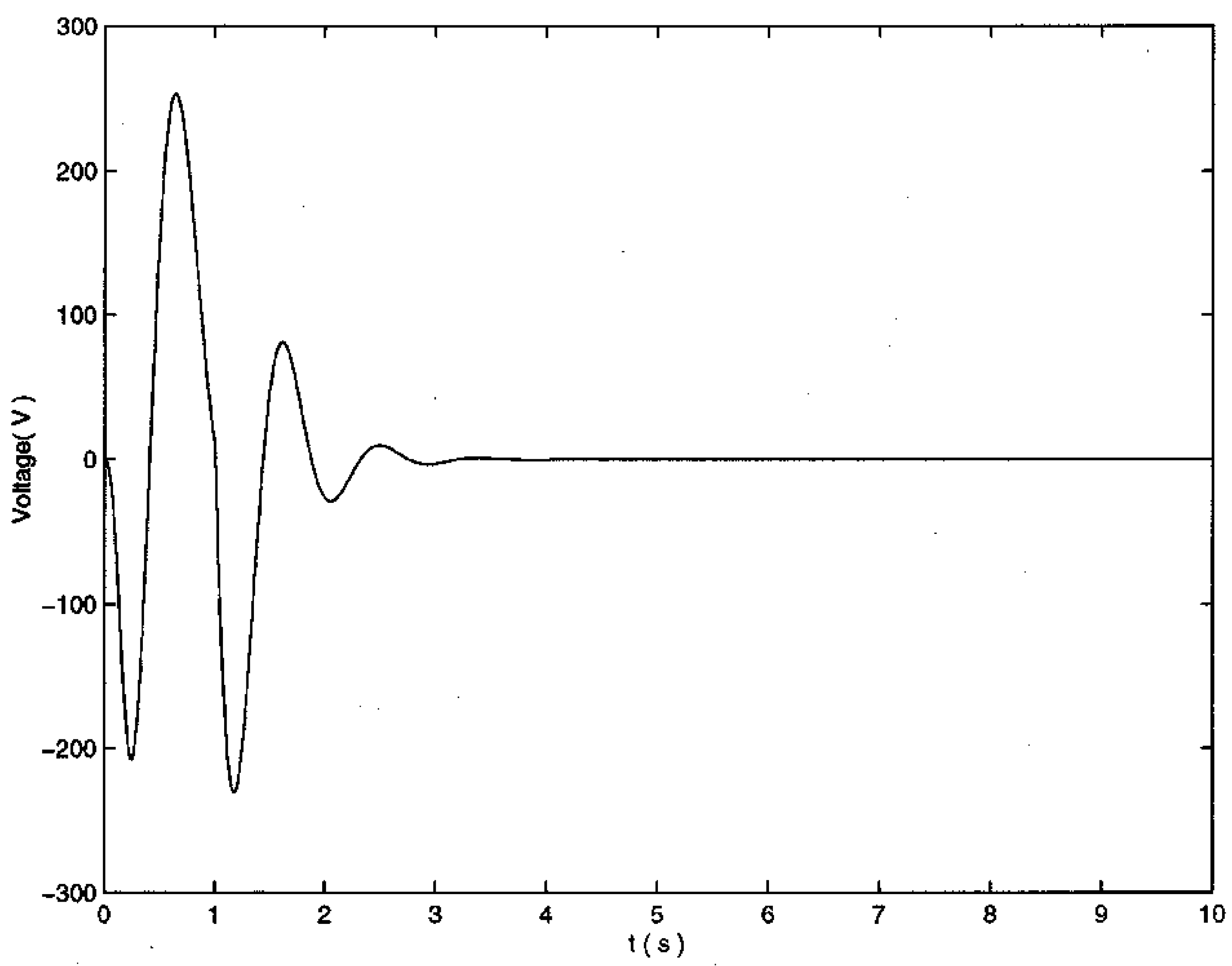

Fig. 5. Voltage control of ANNC.

In fact, we have conducted extensive simulation studies but only one is presented. It is found that, in general, PD control is not sufficient and has residue vibrations for a long time. In addition, high PD gains result large overshoots, and low PD gains lead to slow responses. No matter how to change the gains of PD control, the residue vibrations cannot be suppressed effectively, unless to make the response very slow. On the other hand, the proposed controller can control the system effectively.

Different tracking performance can be achieved by adjusting parameter adaptation gains and other factors, such as the size of the networks. Because neural networks are used to approximate system's functions, the requirements on the initial knowledge of the system is greatly reduced. Though only a single-link smart materials robot is used to simulate the effectiveness of the proposed controller, it can be used to control higher degrees-of-freedom robots as well.

VI. CONCLUSION

In this paper, an adaptive neural network controller for smart materials robots was investigated based on the singular perturbation technique. An adaptive neural network controller has been developed to control the slow subsystem. It was shown that if bounded basis function networks such as Gaussian Radial Basis Function networks are used, uniformly stable adaptation and tracking are achieved. For the fast subsystem, active suppression of the fast variables has been designed through voltage control. Better control performance has been obtained by applying smart materials to the flexible link robot control. The approach proposed is computationally less expensive than control designs based on full dynamic model. Numerical simulation has been used to illustrate the performance of the controller designed using this approach.

APPENDIX

A. Dynamic modeling of smart materials robots

The smart materials robot under study is a flexible link robot where m segmented piezoelectric materials patches are bonded along the link, acting as actuators or sensors for better controller performance. One end of the beam is rigidly attached to the rotor of a motor in the horizontal plane, the tip payload is considered as a point mass. The schematics of the system is shown in Fig. 6 and the notations are defined in the **Nomenclature**.

In this paper, we make the standard assumption of small deflection and that electrical displacement $D(x, t)$ is perpendicular to the beam in the plane of OX_1Y_1. Thus its z component $D_z = 0$. Moreover, due to the small deflection, we have $D_x << D_y$, therefore, we assume that $D_x = 0$. The magnetic field intensity H is perpendicular to the plane OX_1Y_1; consequently, $H_x = H_y = 0$. We will only consider about D_y and H_z in the following discussion.

In order to find the dominant physical properties of the proposed system and simplify the system model, it is assumed that the whole beam is very thin, which means that the deflection w is only a function of x and is independent of the thickness. Furthermore, by choosing the polarization directions of the upper and lower layer of smart materials opposite to each other, D_y in the upper layer is equal to that of the lower layer when the beam is under small deflections. Therefore, no different notation is used here.

For the quantities defined in the **Nomenclature**, we have the following fundamental relationships:

1. Piezoelectric effects:

$$F^S = c^S S - hD \tag{58}$$

$$E = -h^T S + \beta D \tag{59}$$

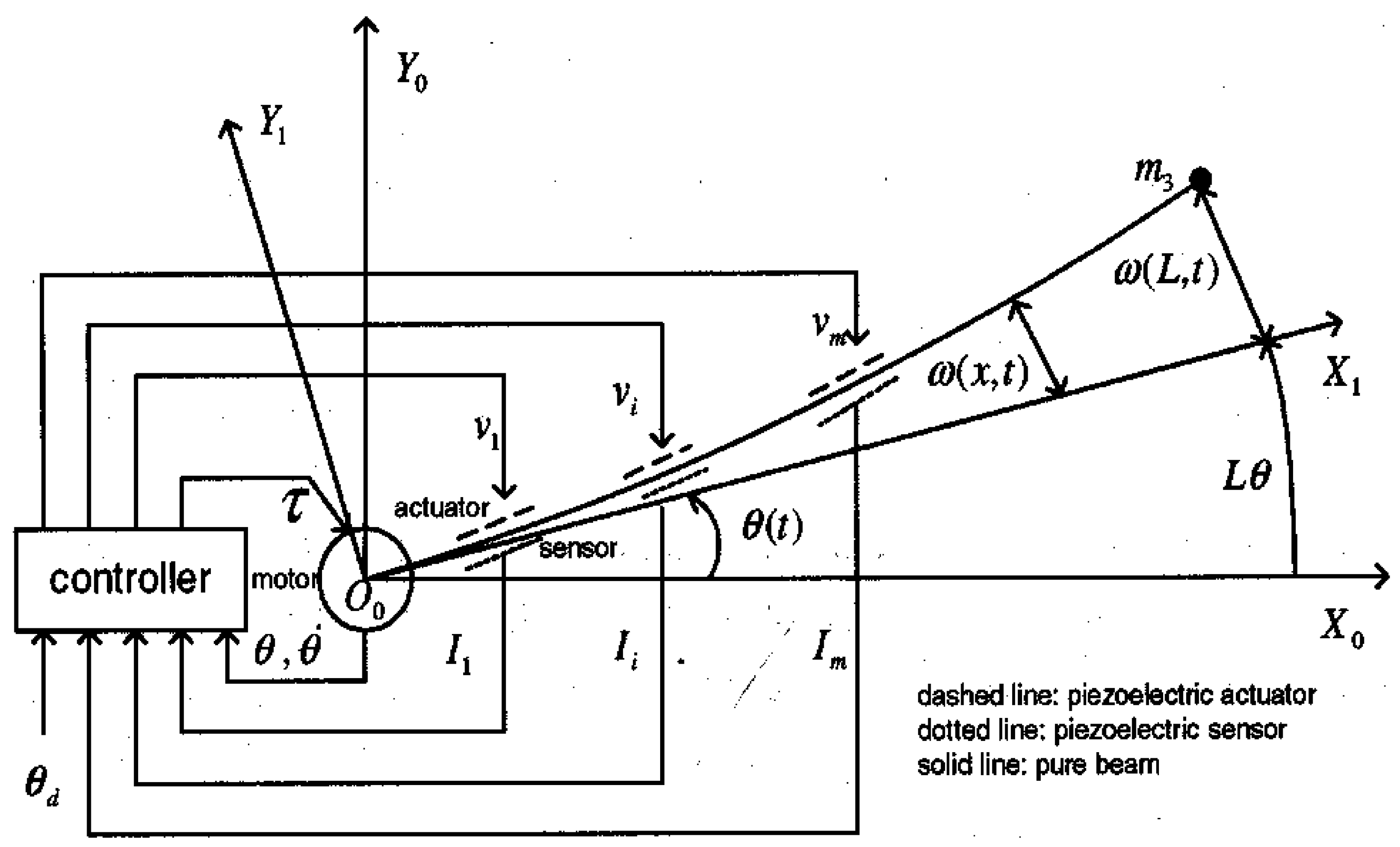

Fig. 6. Smart materials robot system.

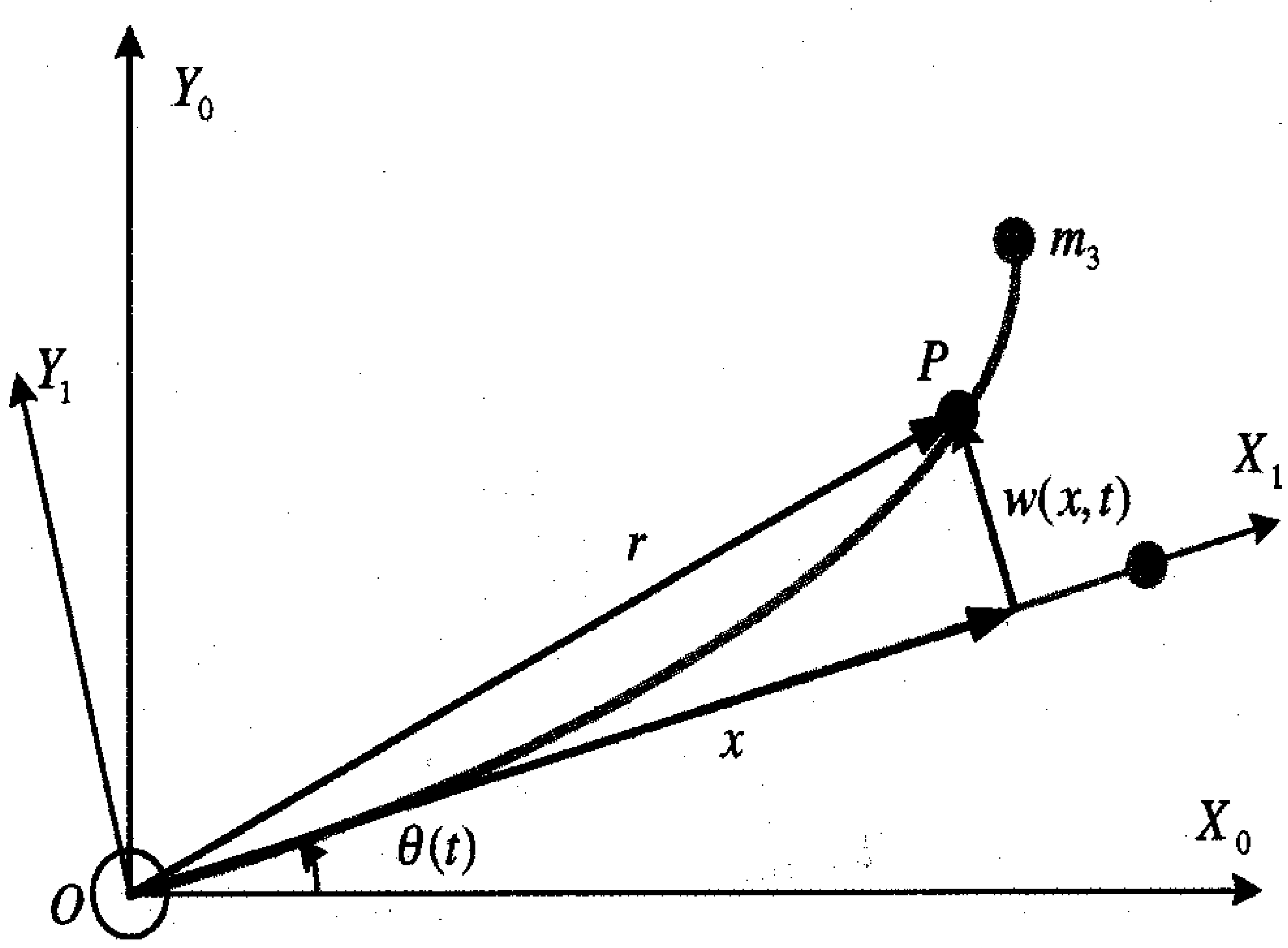

Fig. 7. Detailed diagram of a single-link smart materials robot.

2. Magnetic properties neglecting the piezomagnetic effects:

$$B = \mu H \tag{60}$$

3. Mechanical properties of the pure beam:

$$F^M = c^M S \tag{61}$$

Without loss of generality, we assume that there are m pairs of smart material bonded on the beam from l_{1i} to l_{2i}, $0 \le l_{1i}, l_{2i} \le L$. The system geometry is shown in Fig. 7 The system geometry is shown in Fig. 7.

First, the kinetic energy of the system is derived. The kinetic energy includes mechanical kinetic energy and electrical kinetic energy.

The mechanical kinetic energy is given by

$$E_k{}^M = \frac{1}{2} I_h \dot{\theta}^2 + \int_0^L \frac{1}{2} m_1(x) \dot{r}^T(x,t)\dot{r}(x,t)dx$$

$$+ \sum_{i=1}^{m} \int_{l_{1i}}^{l_{2i}} \frac{1}{2} m_2(x) \dot{r}^T(x,t)\dot{r}(x,t)dx$$

$$= \frac{1}{2} I_h \dot{\theta}^2 + \frac{1}{2}\int_0^L m_1(x)[(-\omega(x,t)\dot{\theta})^2 + (\dot{\theta}x)^2$$

$$+ 2x\dot{\theta}\dot{\omega}(x,t) + \dot{\omega}^2(x,t)]dx$$

$$+ \frac{1}{2}\sum_{i=1}^{m} \int_{l_{1i}}^{l_{2i}} m_2(x)[(-\omega(x,t)\dot{\theta})^2 + (\dot{\theta}x)^2$$

$$+ 2x\dot{\theta}\dot{\omega}(x,t) + \dot{\omega}^2(x,t)]dx \tag{62}$$

where

$$m_1(x) = \begin{cases} ab\rho_1, & 0 \le x < L \\ ab\rho_1 + m_3, & x = L \end{cases}$$

$$m_2(x) = (c_1 + c2)b\rho_2 \tag{63}$$

The first term on the right hand side of equation (62) is the kinetic energy of the hub, the second one is that of the pure beam, and the last one is that of the smart materials.

The electrical kinetic energy, i.e. magnetic energy, is derived as follows.

According to Maxwell equation

$$\nabla \times H = \frac{\partial D}{\partial t} \tag{64}$$

and recalling that $D_x = D_z = 0$, $H_x = H_y = 0$, the equation of H_z can be written as

$$H_z(x,t) = -\int_0^x \dot{D}_y(\xi,t)d\xi \tag{65}$$

where we assumed that $H_z(0, t) = 0$ because of the continuity of magnetic field intensity. We can see that $H_z(x, t)$ is a function of the time derivative of $D_y(x, t)$. Thus, the electrical kinetic energy can be derived as

$$E_k{}^E = \frac{b(c_1+c_2)\mu_{33}}{2} \sum_{i=1}^{m} \int_{l_{1i}}^{l_{2i}} [\int_0^x \dot{D}_y(\xi,t)d\xi]^2 dx$$

$$= \frac{\mu_L}{2} \sum_{i=1}^{m} \int_{l_{1i}}^{l_{2i}} [\int_0^x \dot{D}_y(\xi,t)d\xi]^2 dx \tag{66}$$

The total kinetic energy of the system is the sum of mechanical kinetic energy and electrical kinetic energy, i.e.

$$E_k = E_k{}^M + E_k{}^E \tag{67}$$

Potential energy includes three parts: the mechanical one, the electrical one and the coupled one.

The strain is in order

$$S_1=-y\frac{\partial^2 w(x,t)}{\partial x^2}$$

$$S_2=S_3=S_4=S_5=S_6=0$$

Hence, the total potential energy is given by

$$E_p=\frac{1}{2}b\sum_{i=1}^{m}\int_{l_{1i}}^{l_{2i}}\int_{-\frac{a}{2}-c_2}^{-\frac{a}{2}}[S^TF^S+E^TD]dydx$$

$$+\frac{1}{2}b\int_0^L\int_{-\frac{a}{2}}^{\frac{a}{2}}S^TF^Mdydx$$

$$+\frac{1}{2}b\sum_{i=1}^{m}\int_{l_{1i}}^{l_{2i}}\int_{\frac{a}{2}}^{\frac{a}{2}+c_1}[S^TF^S+E^TD]dydx$$

$$=\frac{c_{L1}}{2}\int_0^L[\frac{\partial^2\omega(x,t)}{\partial x^2}]^2dx+\frac{c_{L2}}{2}\sum_{i=1}^{m}\int_{l_{1i}}^{l_{2i}}[\frac{\partial^2\omega(x,t)}{\partial x^2}]^2dx$$

$$+\frac{\beta_L}{2}\sum_{i=1}^{m}\int_{l_{1i}}^{l_{2i}}D_y^2(x,t)dx$$

$$+h_L\sum_{i=1}^{m}\int_{l_{1i}}^{l_{2i}}D_y(x,t)\frac{\partial^2\omega(x,t)}{\partial x^2}dx \tag{68}$$

From equation (68), it can be found that the potential energy includes three parts: the mechanical potential energy, the electrical potential energy and the coupled potential energy.

Similarly, virtual work also includes the mechanical one and the electrical one. The mechanical virtual work done by the applied force is in the form

$$\delta W^M=\tau\delta\frac{\partial\omega(0,t)}{\partial x}+\tau\delta\theta \tag{69}$$

The electrical virtual work done by the applied voltage is

$$\delta W^E=\sum_{i=1}^{m}\int_{l_{1i}}^{l_{2i}}bV_i(x,t)\delta D_y(x,t)dx \tag{70}$$

The total virtual work is then given by

$$\delta W=\delta W^M+\delta W^E \tag{71}$$

As the main purpose of smart materials is to make a highly integrated smart materials robot with minor changes in the physical properties, according to the AMM modeling in [22], the elastic vibration of the smart materials robot can be expressed as

$$\omega(x,t)=\sum_{i=0}^{\infty}\psi_i(x)q_i(t) \tag{72}$$

where $\psi_i(x)$ are the flexible mode functions and $q_i(t)$ are the generalized coordinates.

And the electrical displacement is of the form

$$D_y(x,t)=\sum_{i=1}^{\infty}-\frac{h_L}{\beta_L}\psi_i''(x)q_i(t) \tag{73}$$

It is well known that the first several modes are dominant in describing the system dynamics, the infinite series can be truncated into a finite one, i.e.,

$$\omega(x,t)=\sum_{i=0}^{nf}\psi_i(x)q_i(t)\quad 0\le x\le L$$

$$D_y(x,t)=\sum_{i=1}^{nf}-\frac{h_L}{\beta_L}\psi_i''(x)q_i(t)\quad 0\le x\le L \tag{74}$$

Define the generalized coordinates vector as

$$q=[\theta\ q_1\ q_2\ \dots\ q_{nf}]^T \tag{75}$$

From Equations (62), (66), (67), (72) and (73), the kinetic energy of the system is then given by

$$E_k=E_k^M+E_k^E=\frac{1}{2}\dot q^TM\dot q \tag{76}$$

where $M\in R^{(n_f+1)\times(n_f+1)}$ is a symmetric and positive definite inertial matrix.

From (68), (72) and (73), the potential energy of the system can be rewritten as

$$E_P=\frac{1}{2}q^TKq \tag{77}$$

where $K=diag[0,\ K_{ff}]\in R^{(n_f+1)\times(n_f+1}$ is the stiffness matrix.

Considering the boundary condition $\frac{\partial}{\partial x}\delta w(0,t)=0$, we obtain the mechanical virtual work as

$$\delta W^M=F_1^T\delta q \tag{78}$$

where

$$F_1=[\tau,0,\dots,0]^T\in R^{(n_f+1)}$$

Assuming voltage $V_i(x,t)$ does not depend on x_i, we have

$$\delta W^E=F_2^T\delta q \tag{80}$$

where

$$F_2=\begin{bmatrix}0\\F_fw\end{bmatrix}\in R^{(n_f+1)} \tag{81}$$

$$F_f=\begin{bmatrix} -\frac{bh_L}{\beta_L}\int_{l_{11}}^{l_{21}}\psi_1''(x)dx & \cdots & -\frac{bh_L}{\beta_L}\int_{l_{1m}}^{l_{2m}}\psi_1''(x)dx \\ -\frac{bh_L}{\beta_L}\int_{l_{11}}^{l_{21}}\psi_2''(x)dx & \cdots & -\frac{bh_L}{\beta_L}\int_{l_{1m}}^{l_{2m}}\psi_2''(x)dx \\ \cdots & & \\ -\frac{bh_L}{\beta_L}\int_{l_{11}}^{l_{21}}\psi_N''(x)dx & \cdots & -\frac{bh_L}{\beta_L}\int_{l_{1m}}^{l_{2m}}\psi_N''(x)dx \end{bmatrix}\in R^{n_f\times m} \quad (82)$$

$w=[\,V_1\ V_2\ \ldots\ V_m]^T\in R^m$ is the vector of control voltages (83)

and F_f is full row rank which is assured by the configuration of the smart materials robot.

Applying the Euler-Lagrange equation

$$\frac{d}{dt}\frac{\partial L}{\partial \dot{q}_i}-\frac{\partial L}{\partial q_i}=F_i$$

the dynamic equation of the whole system can be obtained as

$$M(q)\ddot{q}+C(q,\dot{q})\dot{q}+Kq=F_1+F_2 \quad (84)$$

According to Equations (79) and (81), we have

$$F_1+F_2=Fu \quad (85)$$

where

$$F=\begin{bmatrix} I & 0\\ 0 & F_f\end{bmatrix}$$

$$u=[\tau\ \ w]^T \quad (86)$$

It can be seen that the generalized force u includes two parts, one part is the joint control torque τ which enters the system through only rigid subsystem, another part is the control voltage w which enters the system through only the fast subsystem. This property will greatly facilitate the Singular Perturbation analysis in the paper.

Subsequently, the dynamic model of smart materials robot can be expressed as

$$M(q)\ddot{q}+C(q,\dot{q})\dot{q}+Kq=F_u \quad (87)$$

where $M(q)$ is the symmetric positive definite inertia matrix; $C(q,\dot{q})\dot{q}$ represents the Coriolis and Centrifugal forces, and K is the stiffness matrix of the smart materials robot.

NOMENCLATURE

a	thickness of the beam
b	width of the beam and that of the smart materials
$B\in R^3$	magnetic flux density vector
$c^M\in R^{6\times 6}$	symmetric matrix of elastic stiffness coefficients of the pure beam
$c^S\in R^{6\times 6}$	symmetric matrix of elastic stiffness coefficients of the smart materials
c_1	thickness of upper surface smart materials patch
c_{11}^M	stiffness of the pure beam
c_{11}^s	stiffness of the piezoelectric materials
c_2	thickness of lower surface smart materials patch
$c_{L1}=\frac{c_{11}^M a^3 b}{12}$	stiffness per unit length of the pure beam
$c_{L2}=\frac{c_{11}^s b}{3}[(\frac{a}{2}+c_1)^3+(\frac{a}{2}+c_2)^3-\frac{a^3}{4}]$	stiffness per unit length of the smart materials
$D(x,t)\in R^3$	electrical displacement at location x and time t
E_k	system kinetic energy
E_p	system potential energy
$E\in R^3$	electrical field intensity vector
$F^M\in R^6$	simplified stress vector of the pure beam
$F^S\in R^6$	simplified stress vector of the smart materials
$h\in R^{6\times 3}$	coupling coefficients matrix
h_{12}	coupling parameter per unit volume of the piezoelectric material
$h_L=\frac{1}{2}h_{12}b(c_1-c_2)(c_1+c_2+a)$	coupling parameter per unit length of the smart materials robot
$H(x,t)\in R^3$	magnetic field intensity at location x and time t
I_h	inertia of the hub
L	length of the beam
m_3	tip payload
r	position vector of point P expressed in the fixed-base frame
$S\in R^6$	simplified strain vector
$V(x,t)$	voltage applied to the piezoelectric actuator
W	virtual work done by non-conservative forces
OX_1Y_1	local reference frame with axis OX_1 tangential to the beam at the base
OX_0Y_0	fixed base frame
$\beta\in R^{3\times 3}$	symmetric matrix of impermittivity coefficients
β_{22}	impermittivity per unit volume of the piezoelectric material
$\beta_L=b(c_1+c_2)\beta_{22}$	impermittivity per unit length of the smart materials robot

$\omega(x, t)$ deflection at location x and time t
$\theta(t)$ joint angle at the hub
$\theta_d(t)$ desired joint angular trajectory
$\mu \in R^{3\times3}$ permeability coefficients matrix
μ_{33} permeability of the piezoelectric material
$\mu_L = \beta(c_1 + c_2)\mu_{33}$ permeability per unit length of the smart materials robot
ρ_1 mass per unit volume of the pure beam
ρ_2 mass per unit volume of the smart materials
$\rho_{L1} = ab\rho_1$ mass per unit length of the pure beam
$\rho_{L2} = (c_1 + c_2)b\rho_2$ mass per unit length of the smart materials
$\tau(t)$ torque applied to the base of the manipulator

REFERENCES

1. Cannon, R.H. Jr. and E. Schmitz, "Initial Experiments on the End-point Control of a Flexible Robot," *Int. J. Rob. Res.*, Vol. 3, No. 3, pp. 62-75 (1984).
2. Arakawa, A., T. Fukuda and F. Hara, "H_∞ Control of a Flexible Robotics Arm (Effec of Parameter Uncertainties on Stability)," *IEEE/RSJ Int. Workshop Intell. Rob. Syst. IROS'91*, pp. 959-964 (1991).
3. Chen, Y.P. and K.S. Yeung, "Regulation of a one-link Flexible Robot Arm Using Sliding -Mode Technique, " *Int. J. Contr.*, Vol. 49, pp. 1965-1978 (1989).
4. Luo, Z.H. "Direct Strain Feedback Control of Flexible Robot Arm: New Theoretical and Experimental Results," *IEEE Trans. Automat. Contr.*, Vol. 38, No. 11, pp. 1610-1622 (1993).
5. Ge, S.S., T.H. Lee and G. Zhu, "Energy-Based Robust Controller Design for Multi-link Flexible Robots," *Mechatronics*, Vol. 6, No. 7, pp. 779-798 (1996).
6. Siciliano, B. and W.J. Book, "A Singular Perturbation Approach to Control of Lightweight Flexible Manipulator," *Int. J. Rob. Res.*, Vol. 7, No. 4, pp. 79-89 (1988).
7. Sciavicco, L. and B. Siciliano, *Modeling and Control of Robot Manipulators*, The McGraw-Hill, New York (1996).
8. Tang, Y., M. Tomizuka and G. Guerrero, "Robust Control of Rigid Robots," *Proc. 36th IEEE Conf. Decis. Contr.*, San Diego, Vol. 1, pp. 791-796 (1996).
9. Spong, M.W. and R. Ortega, "On Adaptive Inverse Dynamics Control of Rigid Robots," *IEEE Trans. Automat. Contr.*, Vol. 35, No. 1, PP. 92-95 (1990).
10. Crawley, E.F. and J. Luis, "Use of Piezoelectric Actuators as Elements of Intelligent Structures," *AIAA J.*, Vol. 25, No. 10, pp. 1373-1385 (1987).
11. Baily, T. and J.E. Hubbard, "Distributed Piezoelectric-Polymer Active Vibration Control of a Cantilever Beam," *J. Guid. Dyn. Contr.*, Vol. 8, No. 5, pp. 605-611 (1985).
12. Varadan, V.K., S.Y. Hong and V.V. Varadan, "Piezoelectric Sensors and Actuators for Active Vibration Damping Using Digital Control," *Proc. IEEE Ultrasonics Symp.*, Honolulu, HI, pp. 1211-1214 (1990).
13. Ge, S.S. and T.H. Lee, "Parallel Adaptive Neural Network Control of Robots," *Proc. Inst. Mech. Eng., J. Syst. Contr. Eng.*, Vol. 208, pp. 231-237 (1994).
14. Ge, S.S. and I. Postlethwaite, "Adaptive Neural Network Controller Design for Flexible Joint Robots Using Singular Perturbation Technique," *Trans. The Inst. Meas. Contr.*, Vol. 17, No. 2, pp. 120-131 (1995).
15. Ge, S.S. and T.H. Lee and C.J. Harris, *Adaptive Neural Network Control of Robot Manipulators*, World Scientific, River Edge, NJ (1998).
16. Lewis, F.L., S. Jagannathan and A. Yesildirek, *Neural Network Control of Robots Manipulators and Nonlinear Systems*, Taylor and Francis, London (1999).
17. Poggio, T. and F. Girosi, "A Theory of Networks for Approximation and Learning," Artificial Intelligence Laboratory Memorandum, No. 1140, Massachusetts Institute of Technology, Cambridge, MA (1989).
18. Poggio, T. and F. Girosi, "Networks for Approximation and Learning," *Proc. IEEE*, Vol. 78, pp. 1481-1497 (1990).
19. Zhu, G., *Modelling and Control of Flexible Robots*, Ph.D. Thesis, National University of Singapore (1997).
20. James, M. Ortega, *Matrix Theory, A Second Course*, Plenum Press, New York (1987).
21. Yigit, A.S., "On the Stability of PD Control for a Two-link Rigid-Flexible Manipulator," *ASME J. Dyn. Syst. Meas. Contr.*, Vol. 116, pp. 179-185 (1994).
22. Ge, S.S., T.H. Lee and J.Q. Gong, "Dynamic Modeling of a Smart Materials Robot," *AIAA J.*, Vol. 36, No. 8, pp. 1466-1478 (1998).

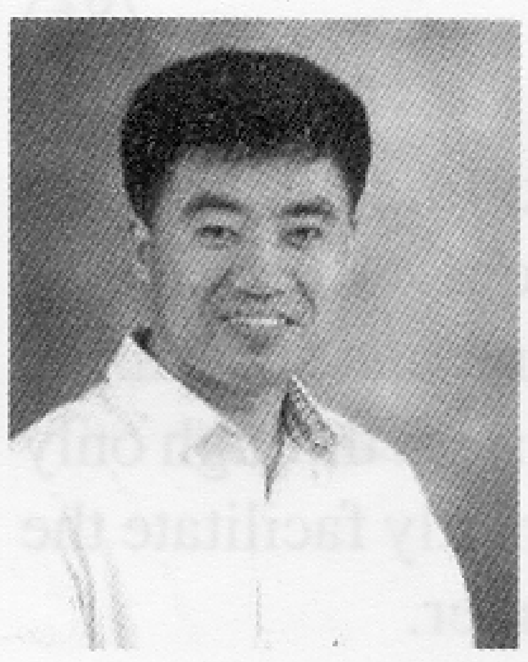

S.S. Ge received the B.Sc. degree from Beijing University of Aeronautics and Astronautics (BUAA), Beijing, China, in 1986, and the Ph. D. degree and the Diploma of Imperial College (DIC) from Imperial College of Science, Technology and Medicine, University of London, in 1993. From May 1992 to June 1993, he did his postdoctoral research at Leicester University, England. He has been with the Department of Electrical & Computer Engineering, the National University of Singapore since 1993, and is currently as an Associate Professor. He was a visiting staff in Laboratoire de' Automatique de Grenoble, France in 1996, the University of Melbourne, Australia in 1998, 1999, and University of Petroleum, China in 2001. He has authored and co-authored over 100 international journal and conference papers, one monograph and co-invented one patent. He served as an Associate Editor on the Conference Editorial Board of the IEEE Control Systems

Society in 1998 and 1999, has been serving as an Associate Editor, IEEE Transactions on Control Systems Technology since June 1999, and a Member of the Technical Committee on Intelligent Control of the IEEE Control System Society since 2000. He was the winner of the 1999 National Technology Award, Singapore. He serves as a technical consultant local industry. He is currently a Senior Member of IEEE. His current research interests are Control of nonlinear systems, Neural Networks and Fuzzy Logic, Robot Control, Real-Time Implementation, Path Planning and Sensor Fusion.

T.H. Lee received the B.A. degree with First Class Honours in the Engineering Tripos from Cambridge University, England, in 1980; and the Ph.D. degree from Yale University in 1987. He is a tenured Professor in the Department of Electrical and Computer Engineering at the National University of Singapore. He is also currently Head of the Drives, Power and Control Systems Group in this Department, and the Vice-Dean (Research) in the Faculty of Engineering. Dr. Lee's research interests are in the areas of adaptive systems, knowledge-based control and intelligent mechatronics. He has published extensively in these areas, and currently holds Associate Editor appointments in Automatica; the IEEE Transactions in Systems, Man and Cybernetics; Control Engineering Practice (an IFAC journal); the International Journal of Systems Science (Taylor and Francis, London); and Mechatronics journal (Oxford, Pergamon Press). Dr. Lee was a recipient of the Cambridge University Charles Baker Prize in Engineering.

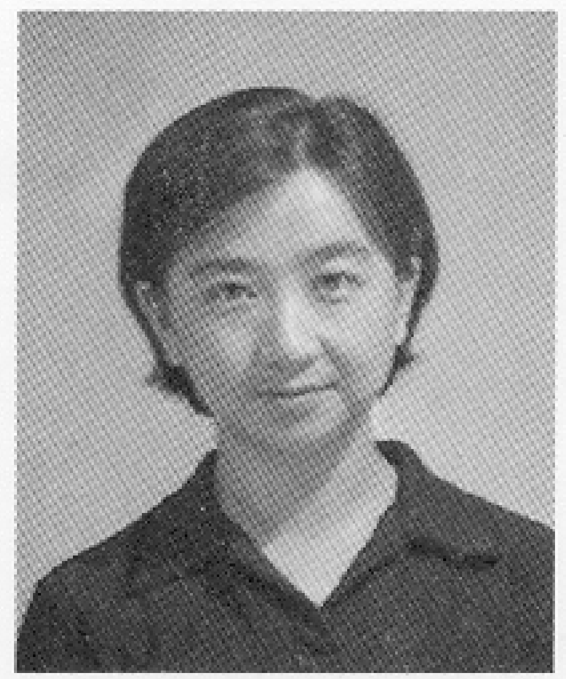

Zhuping Wang received the B.Eng. and the M.Eng. in Department of Automatic Control in 1994 and 1997, respectively, both from Northwestern Polytechnic University, P.R. China. She is now pursuing Ph.D. Degree at Center for Intelligent Control, Department of Electrical & Computer Engineering, National University of Singapore, under the guidance of A/P. S.S. Ge and Prof. T.H. Lee. Her research interests include dynamic modeling and control of flexible link robots/smart materials robots, adaptive nonlinear control, neural network control and robust control.